JOURNAL OF GEOPHYSICAL RESEARCH, VOL. 102, NO. B4, PAGES 8269–8283, APRIL 10, 1997

Improving local earthquake locations using the L1 norm and waveform cross correlation: Application to the Whittier Narrows, California, aftershock sequence

Peter M. Shearer
Institute of Geophysics and Planetary Physics, Scripps Institution of Oceanography
University of California, San Diego, La Jolla

Abstract. Experiments with different earthquake location methods applied to aftershocks of the October 1, 1987, Whittier Narrows earthquake in California (M_L=5.9) suggest that local event locations can be greatly improved through the use of the L1 norm, station corrections and waveform cross correlation. The Whittier Narrows sequence is a compact cluster of over 500 events at 12 to 18 km depth located within the dense station coverage of the Southern California Seismic Network (SCSN), a telemetered network of several hundred short-period seismographs. SCSN travel time picks and waveforms obtained through the Southern California Earthquake Center are examined for 589 earthquakes between 1981 and 1994 in the vicinity of the mainshock. Using a smoothed version of the standard southern California velocity model and the existing travel time picks, improved location accuracy is obtained through use of the L1 norm rather than the conventional least squares (L2 norm) approach, presumably due to the more robust response of the former to outliers in the data. A large additional improvement results from the use of station terms to account for three-dimensional velocity structure outside of the event cluster. To achieve greater location accuracy, waveforms for these events are resampled and low-pass filtered, and the P and S wave cross-correlation functions are computed at each station for every event pair. For those events with similar waveforms, differential times may be obtained from the cross-correlation functions. These times are then combined with the travel time picks to invert for an adjusted set of picks that are more consistent than the original picks and include seismograms that were originally unpicked. Locations obtained from the adjusted picks show a further improvement in accuracy. Location uncertainties are estimated using a bootstrap technique in which events are relocated many times for sets of picks in which the travel time residuals at the best fitting location are used to randomly perturb each pick. Improvements in location accuracy are indicated by the reduced scatter in the residuals, smaller estimated location errors, and the increased tendency of the locations to cluster along well-defined fault planes. Median standard errors for the final inversion are 150 m in horizontal location and 230 m in vertical location, although the relative locations within localized clusters of similar events are better constrained. Seismicity cross sections resolve the shallow dipping fault plane associated with the mainshock and a steeply dipping fault plane associated with a M_L=5.3 aftershock. These fault planes appear to cross, and activity began on the secondary fault plane prior to the large aftershock.

Introduction

Locating earthquakes is one of the oldest problems in seismology and remains an area of active research. The problem is complicated by the nonlinear dependence of seismic travel times on location, the often incomplete knowledge of the full three-dimensional velocity structure along the source-receiver paths, and difficulties associated with inadequate station coverage and outliers in the observed travel time picks. The advent of computers enabled routine event locations for large numbers of events, using one-dimensional reference velocity models and linearized, least squares techniques [e.g., *Flinn*, 1965; *Buland*, 1976]. This made possible the produc-

Paper number 96JB03228.
0148-0227/97/96JB-03228$09.00

tion of both global and local earthquake catalogs listing thousands of events, each located in a standard way.

As computer capabilities improved, researchers began to develop new methods for earthquake location. These include joint-hypocenter-velocity (JHV) inversions to handle the effects of three-dimensional velocity structure [e.g., *Spencer and Gubbins*, 1980; *Pavlis and Booker*, 1980; *Hawley et al.*, 1981; *Thurber*, 1983; *Michael*, 1988; *Eberhart-Phillips*, 1990; *Eberhart-Phillips and Michael*, 1993; *Magistrale and Sanders*, 1996], techniques to downweight the effect of data outliers [e.g., *Anderson*, 1982; *Buland*, 1986; *Kennett*, 1992], station term and master event methods to improve relative location accuracy [e.g., *Douglas*, 1967; *Evernden*, 1969; *Lilwall and Douglas*, 1970; *Frohlich*, 1979; *Jordan and Sverdrup*, 1981; *Smith*, 1982; *Pavlis and Booker*, 1983; *Viret et al.*, 1984; *Pujol*, 1988, 1992, 1995, 1996], grid search, simulated annealing and evolutionary programming approaches to finding global misfit minima [e.g., *Sambridge and Kennett*, 1986; *Sambridge and Gallagher*, 1993; *Billings*, 1994; *Billings et al.*, 1994a; *Minster et al.*, 1995], and waveform cross-correlation techniques to improve locations for clusters of similar events [e.g., *Poupinet et al.*, 1984; *Ito*, 1985; *Fremont and Malone*, 1987; *Xie et al.*, 1991; *Deichmann and Garcia-Fernandez*, 1992; *Got et al.*, 1994; *Nadeau et al.*, 1995; *Haase et al.*, 1995; *Dodge et al.*, 1995; *Gillard et al.*, 1996].

Despite these advances, most events in the standard earthquake catalogs are still located using traditional least squares methods. One reason for this is a desirable conservatism in the production of catalogs, whose value, at least in part, is derived from their consistency, which makes it possible to compare seismicity patterns at different times without the possible biasing effects of a change in the location method. In addition, many techniques that work well on subsets of the data for specialized research projects are not easily implemented into routine production.

As an example, earthquakes in southern California are routinely located by the U.S. Geological Survey and the California Institute of Technology using travel time picks measured by analysts from the over 300 stations of the Southern California Seismic Network (SCSN) [*Wald et al.*, 1995]. Thousands of locations per year are added to the Southern California Catalog of Earthquakes, a list that dates back to 1932. The catalog locations are based on an iterative least squares approach and a standard one-dimensional velocity model. The quality of these routine locations is entirely adequate for public distribution and producing seismicity maps. However, the location uncertainties are often significant, particularly in depth. Improved location accuracy can be achieved by more detailed analyses of seismicity, using station terms, three-dimensional velocity inversions, and/or waveform cross-correlation approaches. This has been done by one or more groups for each major aftershock sequence in southern California in the last 10 years.

While large numbers of events have been relocated to greater accuracy in this way, no standard method has been adopted and much of the seismicity outside of the major aftershock sequences has not been relocated. The research described in this paper is motivated by a desire to develop practical methods for improving earthquake locations in southern California that do not require special data handling or operator intervention and thus can be applied routinely to large parts of the catalog. As a test case, I experiment with locating over 500 aftershocks of the 1987 Whittier Narrows earthquake in the northeastern Los Angeles basin. My results demonstrate that a major improvement in location accuracy can readily be achieved using only the existing travel time picks through the use of the L1 norm and station terms. A further improvement can be achieved by using waveform cross correlation but at considerably greater computational cost.

Whittier Narrows Earthquake

The October 1, 1987, Whittier Narrows earthquake (M_L=5.9) was the largest to occur near Los Angeles since the 1971 San Fernando earthquake. The mainshock focal mechanism, geodetic constraints, and the aftershock distribution indicate that the event occurred on a low-angle northward dipping thrust fault, at a depth of about 15 km [*Hauksson et al.*, 1988; *Hauksson and Jones*, 1989; *Bent and Helmberger*, 1989; *Bolt et al.*, 1989; *Lin and Stein*, 1989]. No surface rupture was found, and the aftershocks were confined to a compact cluster about 6 km in diameter [*Hauksson and Jones*, 1989]. Approximately 600 aftershocks have occurred in the vicinity of the mainshock through 1994. The fairly limited number of aftershocks and their occurrence in a tight cluster near the middle of a dense seismograph network (Figure 1) make the Whittier Narrows sequence ideal for testing the limits of location accuracy.

SCSN catalog locations for the aftershocks are plotted in Figure 2, both in a map view and a south-north cross section. A reference position of 34.06°N, 118.08°W is used in this and subsequent plots. The mainshock and the largest aftershock (M_L=5.3) are indicated with their focal mechanisms. The locations are highly scattered in depth, and the smaller events appear to be systematically located deeper than the larger events. The cause for this bias is not clear but may be related to the lesser number of picks that are generally obtained for the smaller events. In any case, it is apparent that much better location accuracy is required to image the fault plane of the mainshock or even to distinguish between the primary and secondary fault planes.

Hauksson and Jones [1989] performed a detailed study of the aftershocks, relocating them using a custom one-dimensional velocity model as well as computing focal mechanisms for many of the events. The Hauksson and Jones study used data from another network and portable seismic stations to supplement the SCSN data and was able to resolve the fault planes of the mainshock and a M_L=5.3 aftershock. My intention is not to redo this work, which integrates many types of information to examine the complete seismic and tectonic context of the Whittier Narrows event, but rather to

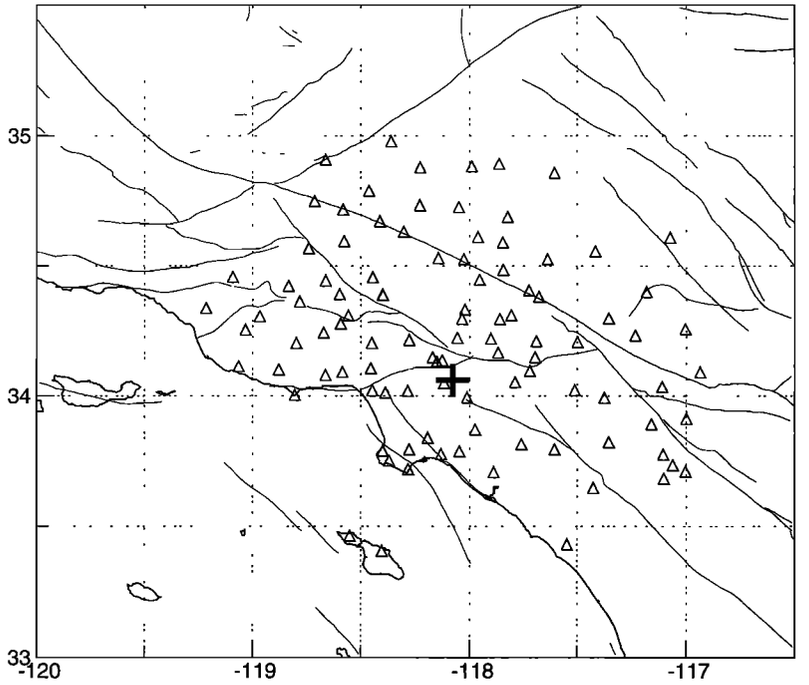

Figure 1. Location of the October 1, 1987, Whittier Narrows mainshock (cross) and the Southern California Seismic Network (SCSN) stations located within 100 km (triangles).

explore the limits of location accuracy that are possible using SCSN data alone, and so might be expected to be readily achievable in other areas.

The SCSN catalog contains 650 events between 1981 and 1994 in a box (34.0 to 34.17°N, 118.17 to 118.0°E) around the Whittier Narrows earthquake. Using only events for which both travel time picks and waveforms are available through the Southern California Earthquake Center (SCEC) reduced this to 589 events; of these, 22 occurred prior to the mainshock. To avoid uncertainties associated with the Pn crossover distance, analysis is restricted to the 111 stations within 100 km of the mainshock where the first arrival is the crustal Pg phase. For these stations the SCSN analysts had picked 8786 P arrivals and 1857 S arrivals, with generally more picks for the larger events. Many seismograms were available from the archive that had not been picked, with a total of 16,138 traces within the range window. My analyses included a small number of events from the December 3, 1988, Pasadena earthquake [i.e., *Jones et al.*, 1990]; I will not describe these here since they are outside the main cluster of events in the Whittier Narrows sequence.

Grid-Search Location Algorithm

As a reference velocity model, I used a smoothed version of the standard southern California velocity model [*Hadley and Kanamori*, 1977; *Wald et al.*, 1995] (Figure 3). The Hadley-Kamamori model divides the crust into three homogeneous layers and has been found to give reasonable fits to average P wave travel times in southern California. However, "layer cake" models of this type are physically unrealistic and predict a series of triplications, large amplitudes on retrograde branches, and sharp corners in the first-arrival travel time curves for Pg. As an alternative, I use a simple model with three linear velocity gradients in the crust that produces a smooth Pg travel time curve that generally agrees with the times predicted by the Hadley-Kanamori model. The advantage of smooth travel time curves for the earthquake location problem is that they can be easily interpolated in range and depth without generating artifacts due to edge effects. With modern computers it is no more difficult to handle smooth crustal models than layered models. A scaled version of the P model is used as a reference S velocity model, assuming a Poisson's ratio of 0.25.

From these models I compute P and S travel time tables at intervals of 2 km in range and source depth. Next, I define a three-dimensional grid of points in a 20-km cube surrounding the mainshock. These points are separated by 1 km, resulting in $21^3 = 9261$ total grid points. I compute ranges to each of the 111 stations from the latitude and longitude of each vertical column of grid points and then obtain predicted P and S travel times from each grid point to each station by interpolating from the travel time tables. The number of grid points is chosen such that this array of travel times fits into the computer memory. Note that the calculation of the travel time array need only be done once and can then be used to locate all of the events within the seismicity cluster.

For each event the observed P and S wave travel time picks are compared to those predicted at each grid point and the best-fitting grid point is located. An equal weighting is assumed between P and S residuals, although there are generally many more P picks. Note

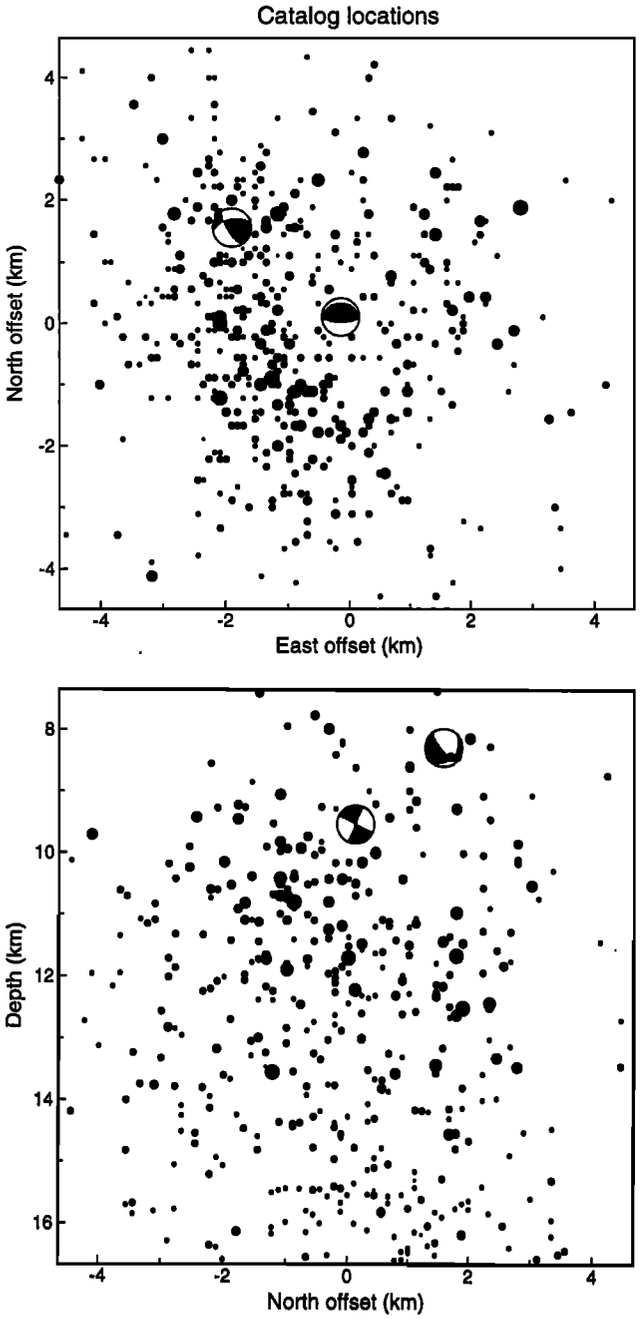

Figure 2. SCSN catalog locations for Whittier Narrows shown in (top) map view and (bottom) S-N cross section relative to a reference location of 34.06°N, 118.08°W. Circle diameter is proportional to event magnitude, except for the two largest events, the M_L=5.9 mainshock (near the center of the top plot) and a M_L=5.3 aftershock, which are indicated by their focal mechanisms as determined by *Hauksson and Jones* [1989].

that a grid search is not required for the earthquake origin time; the best origin time at each grid point may be obtained simply by computing the average (L2 norm) or median (L1 norm) of the residuals. The misfit function in the case of the Whittier Narrows aftershocks varies quite smoothly; thus the grid can be sampled coarsely at first and then at closer intervals once a preliminary location is identified. After the best-fitting grid point is found, the location is further refined by examining a finer grid obtained by interpolating between adjacent grid points. All locations shown in this paper are computed to a nominal resolution of 15 m.

L2 Norm and L1 Norm Solutions

Since the grid-search approach permits a complete sampling of the misfit function, any desired misfit criteria can be applied. Here I experiment with both the L2 norm (conventional least squares, the mean in one-dimensional problems) and the L1 norm (least absolute value, the median in one-dimensional problems). The L2 norm solution is appropriate when the misfit to the travel times is caused by uncorrelated, random Gaussian noise in the picks. Typically, these assumptions are violated in the Earth and the L2 norm may give spurious results due to assigning excessive weight to non-Gaussian outliers in the data. The L1 norm weights residuals more equally in the inversion and is considered more robust with respect to data outliers. The effects of these and other misfit norms on the earthquake location problem were explored by *Anderson* [1982], and the L1 norm was applied to the problem of earthquake location in oceanic regions by *Kennett* [1992].

Locations obtained from the SCSN picks using the L2 norm as a measure of residual misfit are plotted in cross section in Figure 4a. The scatter in the location depths is reduced compared to the catalog locations. Changes in locations are also apparent in the map view; however, to save space, this and subsequent figures will present

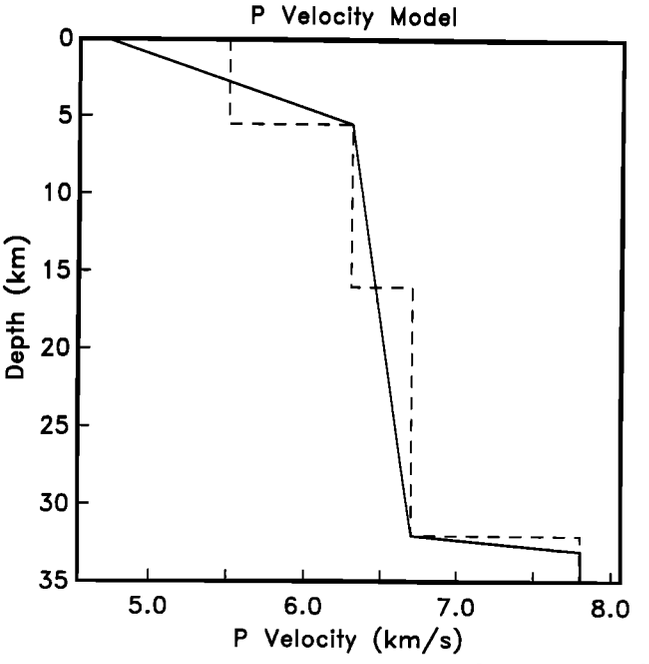

Figure 3. *P* velocity model (solid line) used for the inversions in this paper and the standard southern California velocity model of *Hadley and Kanamori* [1977] (dashed line).

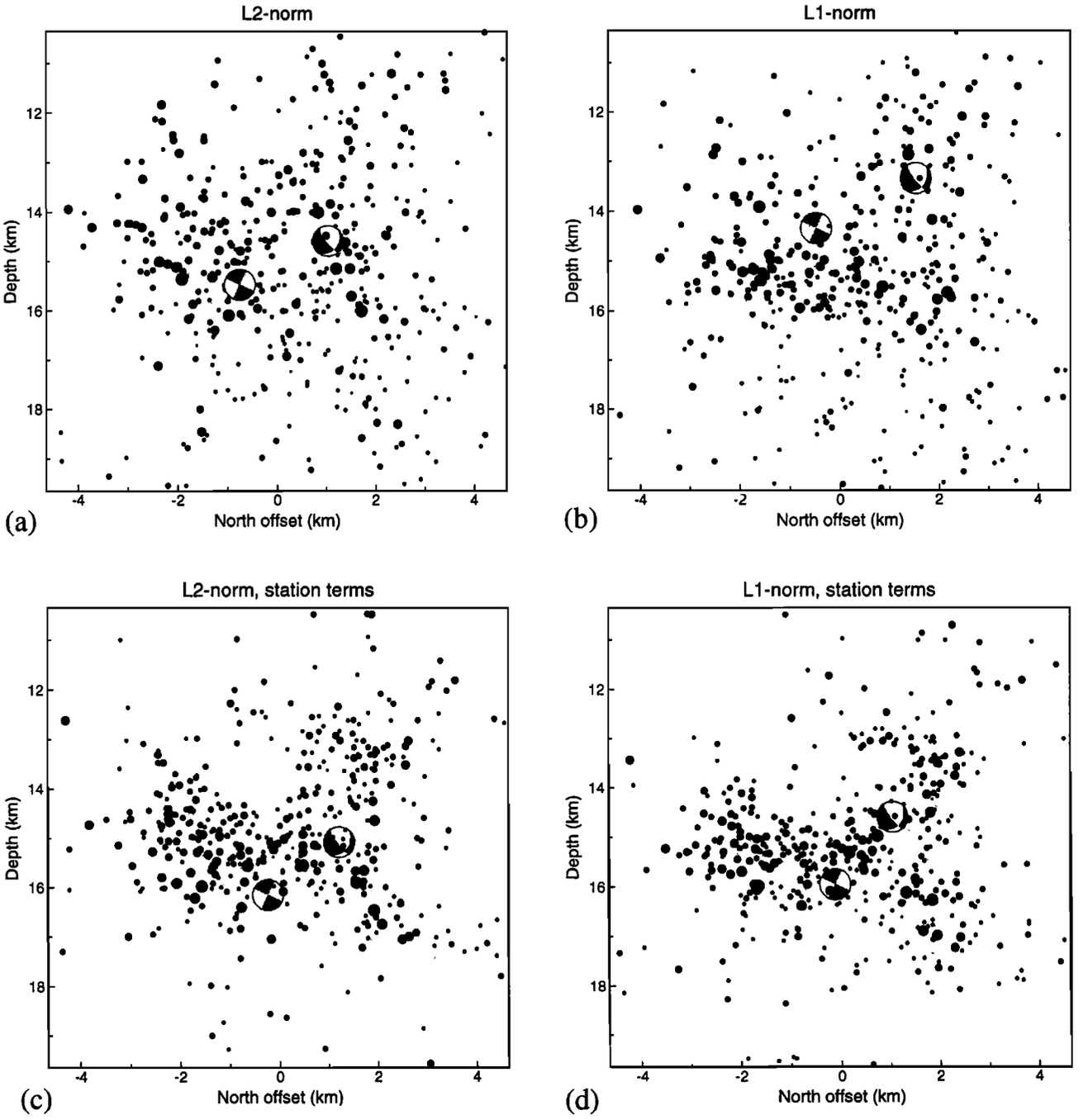

Figure 4. Earthquake locations obtained using (a) an L2 norm measure of misfit (least squares), (b) an L1 norm measure of misfit (least absolute value), (c) the L2 norm with station terms, and (d) the L1 norm with station terms. A S-N cross section is shown relative to a reference location of 34.06°N, 118.08°W. Symbol scaling and focal mechanisms are as in Figure 2. Note the reduced scatter in the locations obtained for the L1 norm solutions.

only the S-N cross section in which the differences between the locations are most pronounced. Figure 4b plots the locations resulting from the L1 norm solution. The L1 norm results show less scatter in depth, with some clustering apparent that is suggestive of the mainshock fault plane. In this and subsequent examples I will use the degree to which the events cluster into well-defined planes as a rough measure of the accuracy of the locations; later I will show that this interpretation is supported by estimates of the standard errors in the locations. For all results presented in this paper the P and S residuals exhibit similar scatter and are weighted equally in the inversions. Locations obtained using only P arrivals are more scattered than those presented here; in this case the advantage of the L1 norm is even more pronounced.

Station Terms

The accuracy of event locations determined using a one-dimensional reference velocity model is limited since three-dimensional velocity variations can introduce systematic biases into the travel times. Locations are improved in joint-hypocenter-velocity inversions [e.g., *Spencer and Gubbins*, 1980; *Pavlis and Booker*, 1980; *Hawley et al.*, 1981; *Thurber*, 1983; *Michael*, 1988; *Eberhart-Phillips*, 1990; *Eberhart-Phillips and Michael*, 1993; *Magistrale and Sanders*, 1996], which solve for a three-dimensional crustal velocity model together with earthquake locations. Lateral velocity variations tend to be strongest at shallow depths, so in many cases, simply including station terms to account for the bias in travel time residuals at each station will lead to significant improvements in the locations. If the source region for the seismicity is small compared to the event-station separation and the scale length of the velocity heterogeneity, then station terms are even more effective since they account for virtually all of the three-dimensional structure along the ray paths. In this case, the effect of station terms in the earthquake location problem will be similar to that of master event methods for determining relative locations [e.g., *Evernden*, 1969; *Jordan and Sverdrup*, 1981].

Plots of residual histograms for the location examples discussed above show that the residuals are highly correlated at individual stations and that much of the scatter in the residuals can be explained with a single offset term at each station. This was implemented using an iterative scheme in which I first located the events and then computed station terms from either the median (for the L1 norm solution) or the mean (for the L2 norm) of the residuals at each station. Next I relocated the events after adjusting the travel times for the station terms, then recomputed the station terms, and so on. This process converges rapidly to a stable solution after only a few iterations. Separate station terms are computed for P and S, and a minimum of five picks are required to compute each station term (final locations are determined only from those picks with associated station terms). The computed station terms for the Whittier Narrows aftershocks are almost all less than 1 s, with no clear range dependence (a range dependence in the station terms would suggest a problem with the reference one-dimensional velocity model).

Determining the best way to calculate station terms and their relationship to location accuracy and three-dimensional velocity variations has been a topic of considerable discussion [e.g., *Douglas*, 1967; *Lilwall and Douglas*, 1970; *Frohlich*, 1979; *Smith*, 1982; *Pavlis and Booker*, 1983; *Pavlis and Hokanson*, 1985; *Viret et al.*, 1984; *Pujol*, 1988, 1992, 1995, 1996]. The method described above is essentially that of *Frohlich* [1979], modified for the grid-search location scheme. My concern here is mostly to improve relative location accuracy between nearby events, for which any self-consistent set of station terms should produce similar results. Improving absolute location accuracy is a more difficult problem, for which there is no easy substitute for full three-dimensional velocity inversions [e.g., *Thurber*, 1992; *Pujol*, 1996].

Figures 4c and 4d show the locations resulting from the L2 and L1 norm methods with station terms. Both sets of locations show much less scatter and greater clustering than before, although the L1 norm solution retains a slight advantage over the L2 norm result. The S-N cross section clearly resolves the gently dipping mainshock fault plane, and there is also better agreement between the aftershock plane and the mainshock location. As I will show later, this apparent improvement in the locations is associated with reduced scatter in the residuals and smaller estimated standard errors. The results presented in Figure 4 show that for Whittier Narrows the L1 norm approach produces locations with significantly less scatter than the more conventional least squares approach. It is possible that a more sophisticated version of the L2 norm approach, in which outliers are iteratively downweighted [e.g., *Buland*, 1986], or other misfit norms [e.g., *Anderson*, 1982], could produce results comparable to the L1 norm solutions. However, there are very few obvious picking errors in the Whittier Narrows travel times, so implementation of such methods might not be straightforward. The primary advantage of the L1 norm approach is its simplicity and the avoidance of any need to specify a scale with which to downweight large residuals.

Waveform Cross-Correlation

The locations plotted in Figure 4d are close to the limit of what can be achieved using the existing picks. Perhaps some improvement could be achieved by careful repicking of the seismograms, but this would be a major task. Three-dimensional velocity inversions would probably produce models that would shift the center position of the cluster (most likely in depth) but would not significantly change the relative locations of the events to each other.

When seismic waveforms are available, cross-correlation techniques can be used to achieve precise relative locations between closely spaced events with similar waveforms [e.g., *Poupinet et al.*, 1984; *Ito*, 1985; *Fremont and Malone*, 1987; *Xie et al.*, 1991; *Deichmann and Garcia-Fernandez*, 1992; *Got et al.*, 1994; *Nadeau et al.*, 1995; *Haase et al.*, 1995; *Dodge et al.*, 1995; *Gillard et al.*, 1996]. This approach is illustrated in Figure 5. Two nearby events will often produce nearly identical waveforms at individual stations, despite the fact that the waveforms vary widely between stations. If the waveforms are similar enough, a time shift can be obtained from the cross-correlation function (or from the phase spectra in frequency domain methods). These differential times are often much more accurate than can be measured by picking individual seismograms and can be used to compute high-precision relative event locations. In many cases, standard location errors of tens of meters or less have been achieved for closely spaced local events.

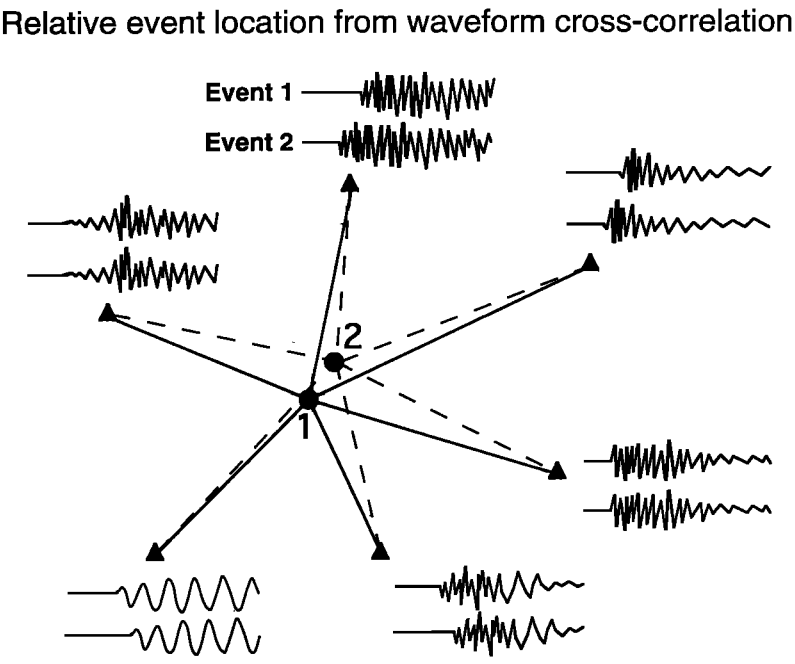

Figure 5. A cartoon showing how waveform cross correlation has been used to improve relative event location. Two closely spaced earthquakes will often produce similar waveforms at individual seismic stations, even though the traces may vary widely between different stations due to local site effects. If the waveforms are similar enough, cross correlation can be used to measure differential times between the events; these times are more accurate than individual arrival times can be picked. These times can then be used to constrain the relative location between the two events.

Despite these successes the waveform cross-correlation approach has generally been used only to relocate small numbers of earthquakes in special areas of interest and has not been applied to large portions of earthquake catalogs. This stems in part from the storage and computational difficulties associated with computing cross-correlation functions for large numbers of events. It is also unclear how similar the earthquakes must be in location and focal mechanism for the method to produce useful results. Does waveform cross correlation work only for small numbers of nearly identical events in tight clusters, or can it be applied more widely to areas of distributed seismicity? To address this question, I experimented with cross-correlating the waveforms from the Whittier Narrows aftershocks.

First, SCSN records available through the SCEC Data Center were extracted for those stations within 100 km of the mainshock, and then windowed from 5 s before the predicted Pg arrival to 5 s after the Sg arrival. The SCSN sample rate increased from 50 to 62.5 Hz in 1983 and fluctuated between 62.5 and 100 Hz between 1986 and 1992 (before stabilizing at 100 Hz). This variable sample rate makes cross correlation inconvenient so I resampled the traces to a uniform 100-Hz sample rate and applied a 10-Hz low-pass filter (the waveform cross correlation works better at lower frequencies). I then computed cross-correlation functions between event pairs, using 3-s windows around the P and S arrivals and time shifts of ± 1.5 s.

Figure 6 illustrates this procedure applied to seven stations for a pair of similar, but not identical, aftershocks. The P arrivals are shown to the left and the S arrivals on the right, together with the computed cross-correlation functions. For most of the stations the waveforms are sufficiently similar that the cross-correlation function has a well-defined peak, representing the time shift between the traces. Since it was not known a priori which event pairs contained similar waveforms, I computed the cross-correlation functions between every event pair. For n events the computation required $n(n-1)/2$ cross correlations per station per phase.

For the 589 Whittier Narrows events this resulted in a total of 173,166 event cross correlations, requiring about a week to compute on a Sparc-4 workstation. Information was saved only for those event pairs with an average waveform correlation coefficient of 0.45 or greater and with at least 10 individual differential times with correlation coefficients of 0.6 or greater. These times could be used to compute differential locations for each event pair and the differential locations then reconciled into a single set of event locations that best fit all of the differential locations. This was the approach used by *Got et al.* [1994], who relocated 250 similar earthquakes within an ~2-km-wide cluster of events at 8 km depth beneath Kilauea volcano in Hawaii. I experimented with this approach for Whittier Narrows but found that the differential locations were sensitive to the assumed absolute event location, which is only loosely constrained by

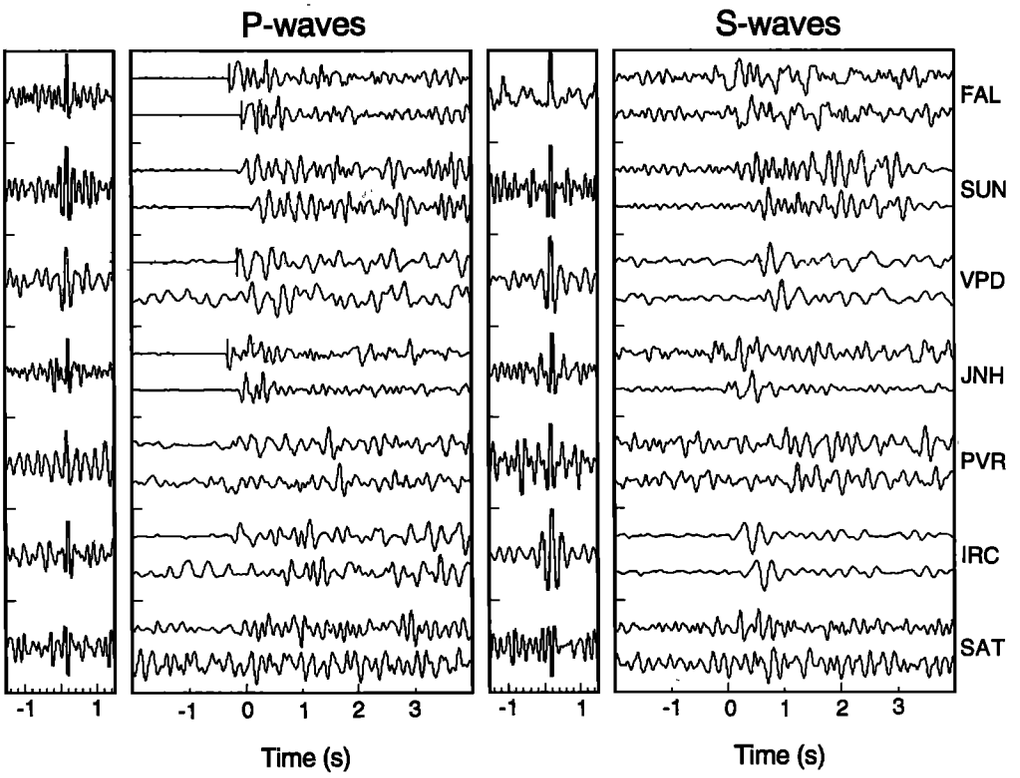

Figure 6. Waveform cross correlation applied to a pair of similar earthquakes, a M_L=2.5 event (October 2, 1987, 0325 UT) and a M_L=2.0 event (October 9, 1987, 0148 UT). The larger boxes show the P and S waves recorded at the seven stations listed at the right. The source-receiver ranges vary from 37 to 45 km; the traces have been low-pass filtered at 10 Hz. The smaller boxes show the cross-correlation functions computed from these data using a 3-s window around the P and S waves. Note that for all of the stations, except for SAT, the cross-correlation function has a well-defined maximum that can be used as a measure of the differential time between the traces.

differential times alone. For distributed sets of events it is inappropriate to assume a single reference location to relocate every event pair. Another difficulty is that relative locations can only be obtained within isolated sets of similar events (termed "multiplets" by Got et al.), making it difficult to image seismicity throughout the entire aftershock sequence.

To avoid these problems, I adopted an alternative approach that combines the differential travel times obtained through waveform cross correlation with the original travel time picks. This is illustrated in Figure 7. For a particular phase (i.e., P or S) and recording station, there are sets of events that are connected by at least one differential time path for a given threshold correlation coefficient; these event clusters are termed "trees" [see *Aster and Scott*, 1993]. Note that not every pair in a tree is required to be correlated; events A, B, and C can form a tree if (A,B) are correlated and (B,C) are correlated, regardless of whether (A,C) are correlated. In addition to the differential times obtained using waveform cross correlation, there are usually travel time picks available for some of the events. My approach in this paper is to solve for a new set of adjusted picks separately for each station that minimize the misfit to both the original picks and the differential times.

We may express the relationship between the observations $\mathbf{d}$ and the model of adjusted picks $\mathbf{m}$ as

$$\mathbf{d} = \mathbf{G}\mathbf{m}$$

or for the specific example shown in Figure 7,

$$\begin{pmatrix} t_1 \\ t_3 \\ t_5 \\ t_6 \\ dt_{12} \\ dt_{23} \\ dt_{24} \\ dt_{45} \\ dt_{46} \\ dt_{56} \end{pmatrix} = \begin{pmatrix} 1 & 0 & 0 & 0 & 0 & 0 \\ 0 & 0 & 1 & 0 & 0 & 0 \\ 0 & 0 & 0 & 0 & 1 & 0 \\ 0 & 0 & 0 & 0 & 0 & 1 \\ 1 & -1 & 0 & 0 & 0 & 0 \\ 0 & 1 & -1 & 0 & 0 & 0 \\ 0 & 1 & 0 & -1 & 0 & 0 \\ 0 & 0 & 0 & 1 & -1 & 0 \\ 0 & 0 & 0 & 1 & 0 & -1 \\ 0 & 0 & 0 & 0 & 1 & -1 \end{pmatrix} \begin{pmatrix} T_1 \\ T_2 \\ T_3 \\ T_4 \\ T_5 \\ T_6 \end{pmatrix}$$

where t_i is the observed travel time pick for event i and dt_{ij} is the observed differential time between events i and j. We seek a model vector $\mathbf{m}$, containing the absolute travel times T, that minimizes the residual vector $\mathbf{d} - \mathbf{G}\mathbf{m}$. To avoid numerical problems associated with large values for t and dt, times can be taken relative to arbitrary reference origin times for each event. This equation is applied separately for P and S waves for each station to times from each event tree. I address this

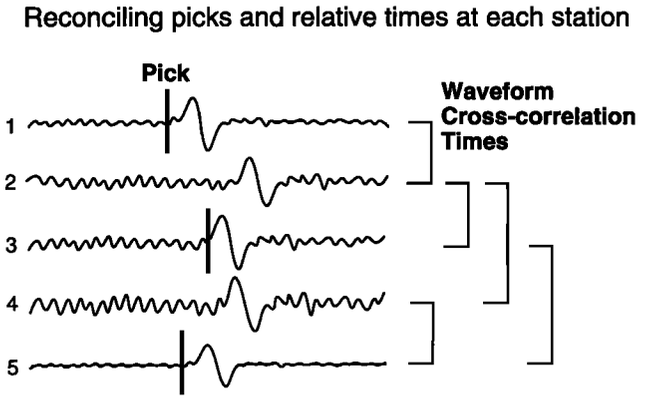

Figure 7. A cartoon illustrating the constraints on the timing of arrivals at a particular seismic station from a "tree" of similar events (a subset of the total number of earthquakes connected by at least one reliable differential time). Some of the individual phases have travel time picks, and some of the possible waveform pairs are similar enough that reliable differential times may be obtained through cross correlation. Both the picked times and the differential times are used to invert for a new set of adjusted picks at each station that is more complete and more consistent than the original set.

problem with an iterative conjugate gradient method, capable of handling very large numbers of observations, with a residual weighting scheme that produces an L1 misfit function (L2 is used for residuals less than 0.1 s to make the algorithm more numerically stable). The method is easily modified to assign error estimates to each observation. The picks and differential times are assigned equal weight for the results presented below; however, generally the differential time information has a dominant effect since there are usually many more differential times than pick times.

In the case where no picks are available for an event tree, the method still returns a solution, but the absolute time is not constrained since an arbitrary constant could be added to the time for each event without affecting the differential times. These "floating trees" are not used in subsequent analysis since they are a fairly small part of the total set of times, although, in principle, they contain information that could be used. Note that this fitting procedure is completely independent of any assumptions about the velocity model or the earthquake locations; it simply provides a way to reconcile absolute and differential travel time information to produce a corrected set of travel time picks. For the case shown in Figure 7 the existing picks are adjusted to be more consistent with the differential time information obtained through waveform cross correlation and picks are obtained for seismograms that were originally unpicked.

As an example, Figure 8 shows the results of this technique applied to a P wave tree of 17 Whittier Narrows aftershocks recorded by station SS2. The SCSN analysts picked P arrival times for 11 of these events; these picks are shown with tic marks on the plot. The dashed line shows the adjusted picks obtained through the inversion procedure; the traces have been aligned on the adjusted picks. In this example it is clear that the adjusted picks are much more consistent that the original picks with respect to the largest pulse in the traces. This is not due to any error by the analyst in assigning picks but, rather, reflects the fact that picks are made from individual seismograms, with noisy and/or emergent arrivals, without reference to traces from other events. Not only are the adjusted picks more consistent with respect to the main arrival pulse, but also picks are now obtained for traces that were originally unpicked. In this example the events are not identical and many individual waveform pairs do not correlate very well, but there are enough similar pairs that the method is able to produce a reasonable alignment of all of the traces. For several traces a weak arrival can be seen earlier than the adjusted pick and it might be argued that the method is producing biased results for these seismograms. It is not clear if the early arrivals result from emergent sources or multipathing in the velocity structure. The problem with attempting to use the true first arrival for these events is that it is very difficult to ensure that it is picked reliably for all stations (with their differing noise levels and site responses). The usefulness of the waveform cross-correlation approach, as applied here and in other studies, is that it consistently aligns the main pulses, producing less scatter in the travel time residuals and the final event locations.

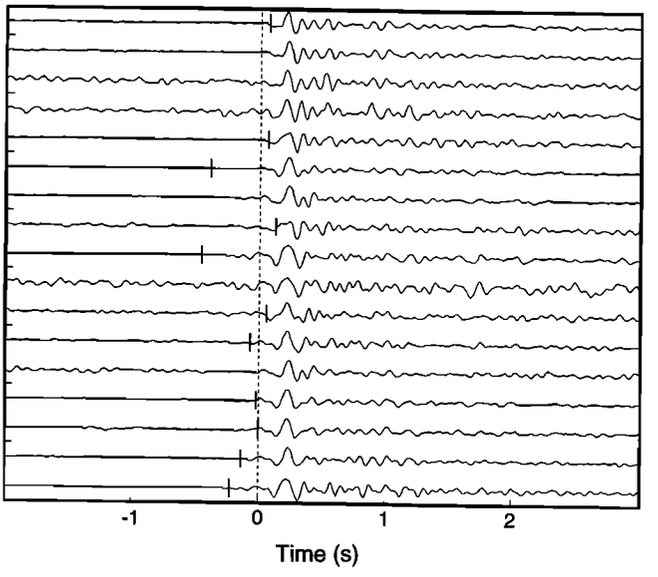

Figure 8. A comparison between the original SCSN P picks for a tree of 17 Whittier Narrows events recorded by station SS2 and the adjusted picks provided by an inversion that included differential times obtained with waveform cross correlation. SCSN picks were available for 11 of the stations and are indicated by tic marks. The waveforms are aligned on their adjusted picks, shown by the dashed line. Note that the adjusted picks are much more consistent and include some seismograms that were originally unpicked.

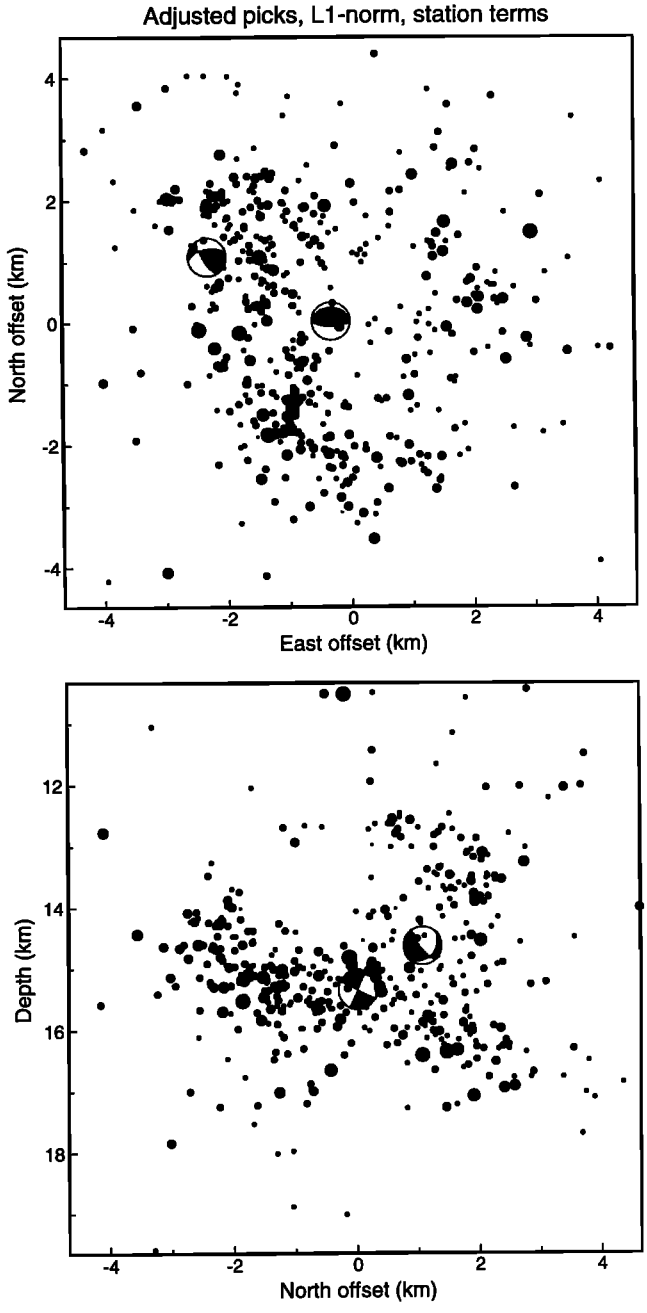

Figure 9. Earthquake locations obtained using the adjusted picks, an L1 norm measure of misfit and station terms in (top) map view and (bottom) cross section, relative to a reference location of 34.06°N, 118.08°W. Symbol scaling and focal mechanisms are as in Figure 2.

The inversion for a new set of adjusted picks is performed separately for each tree and for all stations. This procedure results in a set of 13,394 adjusted P picks and 6862 adjusted S picks for the Whittier Narrows aftershocks, from an original set of 8786 P picks and 1857 S picks. The improvement in the number of S picks is especially helpful, given the small number of original S picks and the importance of S data in constraining earthquake depths [e.g., *Gomberg et al.*, 1990]. Figure 9 shows locations resulting from applying the L1 norm method with station terms to the adjusted picks. The scatter in the locations is reduced, particularly in depth, compared with the result for the original picks (Figure 4d) and the events show a greater tendency to clump into clusters. The mainshock fault plane is well resolved and roughly symmetric about the mainshock hypocenter.

The method described here of incorporating the differential time information into a set of adjusted picks has the following advantages over computing differential locations for each event pair: (1) it is numerically much easier to reconcile the times at each station than to perform a large number of differential locations, (2) the time adjustment procedure is completely independent of the velocity model, (3) the adjusted picks form intermediate results that can be checked to see if the procedure is working correctly, (4) the problem of estimating the best starting locations for the differential locations is eliminated, and (5) the adjusted picks can be used with standard location algorithms, tomographic inversions, etc. The method is particularly suited to the Whittier Narrows aftershocks, a diverse population of events of varying similarity, for which the technique incorporates differential times where appropriate to improve the relative locations between similar events but continues to provide a location for every event (even those that do not cross-correlate with any other events). However, in other cases, particularly tight clusters of very similar events, the differential location approach as described by *Got et al.* [1994] is likely to produce equivalent or even superior results.

Estimating Location Uncertainties

Thus far, I have evaluated the quality of the relocation procedures based upon how well they satisfy the prejudice that the aftershocks should be clustered and grouped into well-defined planar configurations. One may obtain some idea if this is a good assumption by examining the fit to the data that results from each inversion. Define the parameters W_P and W_S as the time difference between the 25th and 75th percentiles in the histogram for the P and S residuals, respectively. Table 1 lists values of W_P and W_S for the different location methods. The largest values of W_P and W_S are found for the L2 norm solution, corresponding to the greatest scatter in the residuals. This scatter is reduced significantly in the L1 norm inversion and drops dramatically when the station terms are included. A small improvement in W_S is noted when the adjusted picks are used (this comparison is made only for the adjusted original picks, not the new picks obtained from the differential times).

Some locations are undoubtedly much better determined than others, and it is desirable to have a measure of this uncertainty. Since the true locations remain unknown, certain assumptions are necessary in order to estimate location accuracy. Classical least squares location methods assume uncorrelated Gaussian random errors and compute error ellipses based upon χ^2

Table 1. Residual Spread and Median Estimated Standard Errors in Location

Location Procedure	W_P, s	W_S, s	$\pm x$, km	$\pm z$, km
L2 norm	0.22	0.27	0.403	0.488
L1 norm	0.17	0.16	0.375	0.474
L2 norm, station corrections	0.08	0.08	0.198	0.250
L1 norm, station corrections	0.06	0.05	0.192	0.241
Adjusted picks, L1 norm, station corrections	0.06	0.04	0.152	0.232

W_P and W_S are the time differences between the 25th and 75th percentiles for P and S wave residuals, respectively; x and z are the median standard errors in horizontal position and depth, respectively.

misfit criteria. These assumptions are often unrealistic and these methods are not easily generalized to other model norms, such as the L1 norm that is used here. As an alternative, I have applied a bootstrap approach, described by *Billings et al.* [1994b], in which random perturbations representing picking errors are added to the travel times and the event is relocated many separate times to obtain an estimate of the probable scatter in the calculated locations due to uncertainties in the picks. This technique has the advantages of fully including all of the nonlinearities in the problem and the fact that some stations and ray paths are much more important than others in constraining the location.

Billings et al. [1994b] applied this method by drawing random picking noise from a Gaussian distribution with a standard deviation appropriate for their data. My approach is somewhat different, in that I use the residuals at the best fitting location for each event as an estimate of the picking errors to be expected (to account for the number of degrees of freedom in the location problem, the residuals are multiplied by the scaling factor $n/(n-4)$, where n is the number of picks). Thus residuals are randomly chosen from the total set of residuals for the event and assigned to the predicted travel times at the best fitting location. The location error estimates are then based upon the scatter in the locations when this process is repeated 200 times. An advantage of this approach is that it naturally produces smaller location error estimates when the misfit to the data is small and larger estimates when the fit to the picks is poor. Due to the $n/(n-4)$ scaling of the residuals, the error estimates may become unrealistically high as n becomes small, an effect first noted by *Evernden* [1969]. However, I did not modify the residual scaling since some conservatism seems desirable in estimating errors for events constrained by small numbers of stations.

I applied this technique to estimate standard errors for each of the aftershock locations. Median standard error estimates are summarized in Table 1 for each location procedure. The median standard error in depth $\pm z$ is consistently greater than the error in horizontal position $\pm x$. Depth standard errors decrease from 490 m for the L2 norm, to 470 m for the L1 norm, to 240 m for the L1 norm with station terms, and to 230 m for the adjusted picks. Note that these location error estimates are based on the consistency of the travel time residuals and are related to random errors in the picks. They do not include the biasing effects of incorrect velocity models or velocity heterogeneity. These factors introduce an additional uncertainty into the absolute location for all of the events; the relative event locations are less affected by incorrect velocity models, particularly when station terms are used.

The improvement in location quality when the adjusted picks are used appears from the plots to be more significant than the small decrease in median estimated errors would suggest (compare Figures 4b and 9). This reflects the fact that much of the reduction in the location scatter is due to an increased tendency for the earthquakes to cluster into tight groups only a few hundred meters in size. These groups generally contain events with similar waveforms and are connected with differential times from the cross-correlation analysis. The relative locations of the events within these groups are tightly constrained, but the relative locations of the subgroups with each other are less well constrained since there are generally fewer differential times available to make connections when the earthquakes are farther apart. Thus most of the improvement in location quality resulting from the waveform cross correlation occurs in the relative location precision at fine scales and does show up in the total estimated errors.

I tested the sensitivity of the solution to variations in the reference one-dimensional velocity model by repeating the final inversion for (1) a smoothed version of the model *Hauksson and Jones* [1989] obtained for the Whittier Narrows sequence and (2) a slowed version of my "standard" model in which the P wave velocities are reduced by 0.3 km/s. The resulting locations showed some distortions, particularly for the slow model, but the overall patterns were similar to those presented here. The slow model is rather extreme, in that it misfits the average travel time versus range; the method was able to accommodate some of the errors in the model with relatively larger station terms for the stations at more distant ranges.

Imaging Two Fault Planes

The mainshock fault plane is well resolved in the S-N cross section in Figure 9, but this projection is oblique

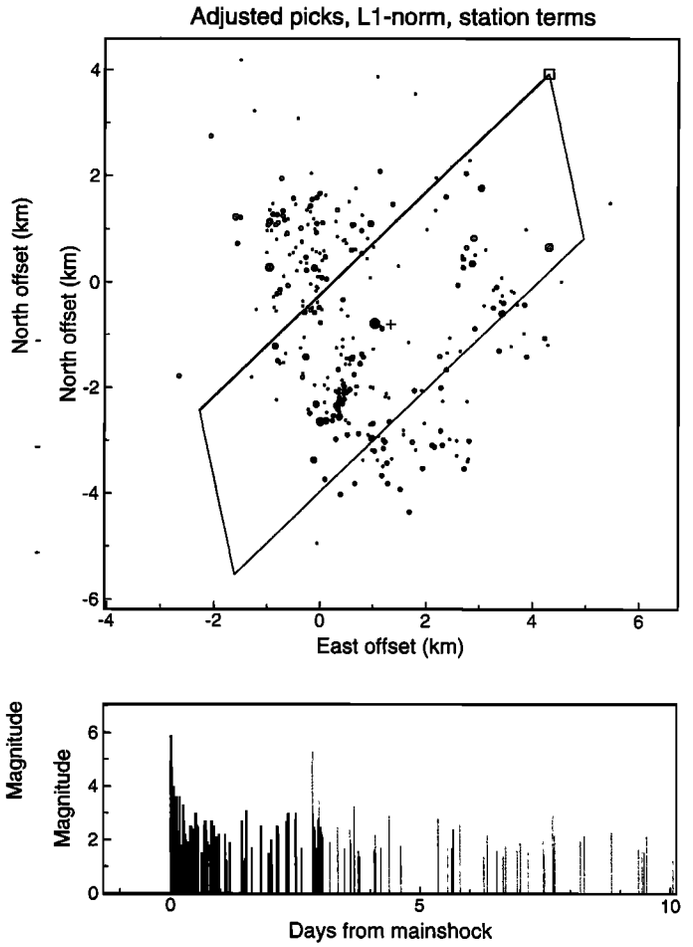

Figure 10. (top) A map view of the final locations, with black indicating events from the mainshock to the large aftershock and gray showing events following the aftershock. The outline of the projection plane for Figure 11 is also shown, with the small square indicating the top right corner of the plane. (bottom) Event magnitude (from the SCSN catalog) versus time.

to the fault plane associated with the M_L=5.3 aftershock. By rotating to a projection plane roughly perpendicular to both faults, one can obtain a better picture of the relationship between the two faults. Figure 10 shows a map view of the seismicity, with the events during the ~3 days between the mainshock and the aftershock shown in black and the events following the aftershock shown in gray. Only events with standard location errors less than 300 m are plotted; this reduces the number of events to 321. This plot also shows an outline of the projection plane used in Figure 11. This projection plane is nearly perpendicular to the two fault planes, indicated by the alignment in the seismicity and the focal mechanisms for the two events. The main fault plane strikes N100°W and dips 20° to the north. The second fault plane strikes N140°E and dips 70° to the SW. Note that the fault planes appear to intersect and that some activity occurred on the second fault plane prior to the aftershock.

The apparent crossing of the fault planes argues against the hypothesis of *Hauksson and Jones* [1989] that the steeply dipping fault plane bounds the edge of the aftershock distribution of the mainshock and that it may have confined the slip of the mainshock. My relocations indicate that the mainshock hypocenter depth is 15.4 km, close to the middle of its aftershock sequence. Hauksson and Jones located the mainshock at a depth of 14.6 km, but obtained shallower depths for almost all of the aftershocks. They suggested that the aftershocks were confined to the hanging wall. My results do not support this interpretation; the aftershocks appear to occur on both sides of the fault.

Most solutions for the mainshock focal mechanism are in general agreement [e.g., *Hauksson and Jones*, 1989; *Bolt et al.*, 1989] and consistent with the aftershock distribution shown in Figure 9. However, *Bent and Helmberger* [1989] proposed that slip may have occurred on two separate faults, with the first event at 15 km depth and a second larger event at 12 km. Although there are hints of nonplanar features in the aftershock locations, there is nothing to suggest separate faults separated by 3 km in depth. Note that the cluster of seismicity at the top of the steeply dipping fault (Figure 11) did not develop until after the large aftershock. Strong motion studies [*Hartzell and Iida*, 1990; *Zeng et al.*, 1993] obtained solutions for slip on a plane that agrees in

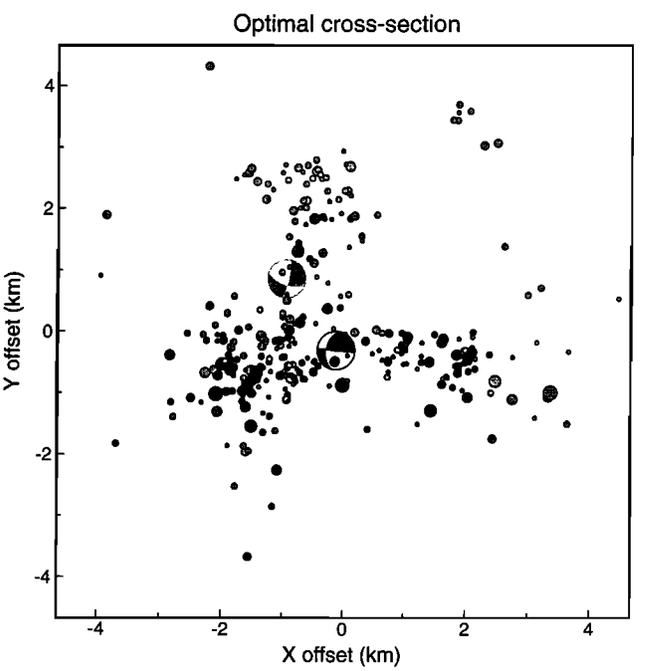

Figure 11. An oblique projection of the final locations onto a plane perpendicular to both the M_L=5.9 mainshock and M_L=5.3 aftershock fault planes. An outline of the projection plane is shown in Figure 10. Only the 321 events with estimated location standard errors less than 300 m are plotted. Events from the mainshock to the large aftershock are shown in black, those following the aftershock are in gray. Note that the seismicity alignments agree with the focal mechanisms and that the two faults appear to cross.

orientation with the aftershock distribution but is significantly larger in the along-strike direction.

Discussion and Future Directions

Seismologists have known for some time that aftershocks tend to occur in the vicinity of the mainshock fault plane; indeed, this is one of the primary methods for distinguishing between the primary and secondary fault planes obtained from the fault plane solution of the mainshock. However, it is less clear the extent to which the aftershocks occur on a single fault or define truly planar features since the typical location uncertainty of several kilometers for local networks blurs the view of the locations. Detailed interpretation of fault geometries and possible fault-fault interactions require more precise locations.

Some indication that the aftershock fault geometries are complicated is provided by focal mechanism studies; in the case of Whittier Narrows, *Hauksson and Jones* [1989] computed focal mechanisms for 59 aftershocks and showed that they indicated a variety of different fault orientations. An analysis of these mechanisms by *Michael* [1991] concluded that they require the presence of a spatially varying stress field. My final locations, plotted in Figure 9, also suggest that the aftershocks are not simply distributed but scatter by about ±500 m off the best-fitting plane and tend to group into compact clusters that hint at other fault alignments. The degree of clustering is important in fractal analyses of earthquake locations; a recent study suggests that the measured fractal dimension for earthquake sequences in California decreases as the location quality improves [*Robertson et al.*, 1995].

A goal of this research has been to identify ways to improve the accuracy of relative event location in southern California using the existing SCSN picks and waveforms. Although my focus here is on the Whittier Narrows aftershocks, the methods and the assumed velocity model are not specific to this sequence and could easily be applied to other regions. I use only travel time picks and waveforms that are already available in standard formats; no additional picking or hand manipulation of the data is required. Compared to the catalog locations, it is clear that substantial improvements in location accuracy are achievable at comparatively little cost by using existing picks and station terms. It should be noted that the deficiencies in the catalog locations are well known and many groups are currently producing improved locations from three-dimensional (3-D) velocity inversions. The advantage of the method described here is that it produces good relative event locations without the complications of a three-dimensional model. While incorporation of a complete 3-D model will certainly improve absolute event locations, most 3-D models are unlikely to produce significant changes in relative event positions within localized regions on the scale of a few kilometers.

Further improvements in location accuracy are possible using waveform cross correlation, whose benefits do not appear to be limited to isolated clusters of very similar events. Large-scale use of the waveforms is computationally more difficult but is within the capabilities of modern workstations. As the number of events increases, the number of possible event pairs scales approximately as n^2. Thus, while it is possible to process every event pair for Whittier Narrows (n=589), this would not be practical for larger California aftershock sequences, such as Landers ($n > 20,000$) or Northridge ($n > 10,000$). However, in these cases it would probably be sufficient to determine differential times between each event and, for example, its 50 closest neighbors. In this case the computation time would scale as $50n$ and much larger problems could be addressed. As shown above, differential times obtained from waveform cross correlation can be used to compute an adjusted set of travel time picks that are capable of producing high-resolution images of earthquake locations. These adjusted picks could also be used in three-dimensional velocity inversions since they are derived independently from any velocity model.

Waveform cross correlation produces information in addition to differential times. For example, the optimal amplitude scaling between traces is provided by the cross-correlation function and could be used to compute differential magnitudes between event pairs. One could then solve for a best fitting magnitude for each event, perhaps obtaining much greater accuracy than the nominal 0.1 precision with which magnitudes are currently listed in earthquake catalogs. I have not yet explored the relationship between event focal mechanism and the degree of waveform similarity. If waveforms remain similar for closely spaced events with different focal mechanisms, differing primarily only in their amplitude and polarity, it might be possible to compute differential focal mechanisms using waveform cross correlation. This would be analogous to a method used by *Ekström and Richards* [1994] to determine source parameters of closely spaced events using surface wave amplitudes.

Acknowledgments. Keith Dinger greatly assisted in this research by extracting the picks and the waveform data for the Whittier Narrows events; he also produced Figure 1. I am grateful to the operators and analysts who maintain the USGS/Caltech Southern California Seismic Network and who pick and archive the seismograms and to the personnel at the Southern California Earthquake Center who distribute the data. Egill Hauksson generously provided a list of his earthquake locations and focal mechanisms. This research was funded by USGS/NEHRP grant 1434-94-G-2454.

References

Anderson, K.R., Robust earthquake location using M-estimates, *Phys. Earth Planet. Inter.*, *30*, 119-130, 1982.

Aster, R.C., and J. Scott, Comprehensive characterization of waveform similarity in microearthquake data sets, *Bull. Seismol. Soc. Am.*, *83*, 1307–1314, 1993.

Bent, A.L., and D.V. Helmberger, Source complexity of the October 1, 1987, Whittier Narrows earthquake, *J. Geophys. Res.*, *94*, 9548–9566, 1989.

Billings, S.D., Simulated annealing for earthquake location, *Geophys. J. Int.*, *118*, 680–692, 1994.

Billings S.D., B.L.N. Kennett, and M.S. Sambridge, Hypocentre location: Genetic algorithms incorporating problem-specific information, *Geophys. J. Int.*, *118*, 693–706, 1994a.

Billings, S.D., M.S. Sambridge, and B.L.N. Kennett, Errors in hypocenter location: Picking, model, and magnitude dependence, *Bull. Seismol. Soc. Am.*, *84*, 1978–1990, 1994b.

Bolt, B.A., A. Lomax, and R.A. Uhrhammer, Analysis of regional broadband recordings of the 1987 Whittier Narrows, California, earthquake, *J. Geophys. Res.*, *94*, 9557–9568, 1989.

Buland, R., The mechanics of locating earthquakes, *Bull. Seismol. Soc. Am.*, *66*, 173–187, 1976.

Buland, R., Uniform reduction error analysis, *Bull. Seismol. Soc. Am.*, *76*, 217–230, 1986.

Deichmann, N., and M. Garcia-Fernandez, Rupture geometry from high-precision relative hypocentre locations of microearthquake ruptures, *Geophys. J. Int.*, *110*, 501–517, 1992.

Dodge, D.A., G.C. Beroza, and W.L. Ellsworth, Foreshock sequence of the 1992 Landers, California, earthquake and its implications for earthquake nucleation, *J. Geophys. Res.*, *100*, 9865–9880, 1995.

Douglas, A., Joint epicentre determination, *Nature*, *215*, 47–48, 1967.

Eberhart-Phillips, D., Three-dimensional P and S velocity structure in the Coalinga region, California, *J. Geophys. Res.*, *95*, 15,343–15,363, 1990.

Eberhart-Phillips, D., and A.J. Michael, Three-dimensional velocity structure, seismicity, and fault structure in the Parkfield region, central California, *J. Geophys. Res.*, *98*, 15,737–15,758, 1993.

Ekström, G., and P.G. Richards, Empirical measurements of tectonic moment release in nuclear explosions from teleseismic surface waves and body waves, *Geophys. J. Int.*, *117*, 120–140, 1994.

Evernden, J.F., Precision of epicentres obtained by small numbers of world-wide stations, *Bull. Seismol. Soc. Am.*, *59*, 1365–1398, 1969.

Flinn, E.A., Confidence regions and error determinations for seismic event location, *Rev. Geophys.*, *3*, 157–185, 1965.

Fremont, M.-J., and S.D. Malone, High precision relative locations of earthquakes at Mount St. Helens, Washington, *J. Geophys. Res.*, *92*, 10,223–10,236, 1987.

Frohlich, C., An efficient method for joint hypocenter determination for large groups of earthquakes, *Comput. Geosci.*, *5*, 387–389, 1979.

Gillard, D., A.M. Rubin, and P. Okubo, Highly concentrated seismicity caused by deformation of Kilauea's deep magma system, *Nature*, *384*, 343–346, 1996.

Gomberg, J.S., K.M. Shedlock, and S.W. Roecker, The effect of S-wave arrival times on the accuracy of hypocenter location, *Bull. Seismol. Soc. Am.*, *80*, 1605–1628, 1990.

Got, J.-L., J. Fréchet, and F.W. Klein, Deep fault plane geometry inferred from multiplet relative relocation beneath the south flank of Kilauea, *J. Geophys. Res.*, *99*, 15,375–15,386, 1994.

Haase, J.S., P.M. Shearer, and R.C. Aster, Constraints of temporal variations in velocity near Anza, California, from analysis of similar event pairs, *Bull. Seismol. Soc. Am.*, *85*, 194–206, 1995.

Hadley, D.M., and H. Kanamori, Seismic structure of the Transverse Ranges, California, *Geol. Soc. Am. Bull.*, *88*, 1461–1478, 1977.

Hartzell, S., and M. Iida, Source complexity of the 1987 Whittier Narrows, California, earthquake from the inversion of strong motion records, *J. Geophys. Res.*, *95*, 12,475–12,485, 1990.

Hauksson, E., and L.M. Jones, The 1987 Whittier Narrows earthquake sequence in Los Angeles, Southern California: Seismological and tectonic analysis, *J. Geophys. Res.*, *94*, 9569–9589, 1989.

Hauksson, E., et al., The 1987 Whittier Narrows earthquake in the Los Angeles metropolitan area, California, *Science*, *239*, 1409–1412, 1988.

Hawley, B.W., G. Zandt, and R.B. Smith, Simultaneous inversion for hypocenters and lateral velocity variations: An iterative solution with a layered model, *J. Geophys. Res.*, *86*, 7073–7086, 1981.

Ito, A., High resolution relative hypocenters of similar earthquakes by cross-spectral analysis method, *J. Phys. Earth*, *33*, 279–294, 1985.

Jones, L.M., K.E. Sieh, E. Hauksson, and L.K. Hutton, The 3 December 1988 Pasadena, California earthquake: Evidence for strike-slip motion on the Raymond fault, *Bull. Seismol. Soc. Am.*, *80*, 474–482, 1990.

Jordan, T.H., and K.A. Sverdrup, Teleseismic location techniques and their application to earthquake clusters in the south-central Pacific, *Bull. Seismol. Soc. Am.*, *71*, 1105–1130, 1981.

Kennett, B.L.N., Locating oceanic earthquakes—The influence of regional models and location criteria, *Geophys. J. Int.*, *108*, 848–854, 1992.

Lilwall, R.C., and A. Douglas, Estimation of P-wave travel times using the joint epicentre method, *Geophys. J. R. Astron. Soc.*, *19*, 165–181, 1970.

Lin, J., and R.S. Stein, Coseismic folding, earthquake recurrence, and the 1987 source focal mechanism at Whittier Narrows, Los Angeles basin, California, *J. Geophys. Res.*, *94*, 9614–9632, 1989.

Magistrale, H., and C. Sanders, Evidence from precise earthquake hypocenters for segmentation of the San Andreas fault in San Gorgonio Pass, *J. Geophys. Res.*, *101*, 3031–3044, 1996.

Michael, A.J., Effects of three-dimensional velocity structure on the seismicity of the 1984 Morgan Hill, California, aftershock sequence, *Bull. Seismol. Soc. Am.*, *78*, 1199–1221, 1988.

Michael, A.J., Spatial variations in stress within the 1987 Whittier Narrows, California, aftershock sequence: New techniques and results, *J. Geophys. Res.*, *96*, 6303–6319, 1991.

Minster, J.-B. H., N.P. Williams, T.G. Masters, J.F. Gilbert, and J.S. Haase, Application of evolutionary programming to earthquake hypocenter determination, in *Evolutionary Programming; Proceedings of the Fourth Annual Conference on EP*, edited by J. McDonnell, MIT Press, Cambridge, pp. 3–17, 1995.

Nadeau, R.M., W. Foxall, and T.V. McEvilly, Clustering and periodic recurrence of microearthquakes on the San Andreas Fault at Parkfield, California, *Science*, *267*, 503–507, 1995.

Pavlis, G.L., and J.R. Booker, The mixed discrete continuous inverse problem: Application to the simultaneous determination of earthquake hypocenters and velocity structure, *J. Geophys. Res.*, *85*, 4801–4810, 1980.

Pavlis, G.L., and J.R. Booker, Progressive multiple event location (PMEL), *Bull. Seismol. Soc. Am.*, *73*, 1753–1777, 1983.

Pavlis, G.L., and N.B. Hokanson, Separated earthquake location, *J. Geophys. Res.*, *90*, 12,777–12,789, 1985.

Poupinet, G., W.L. Ellsworth, and J. Frechet, Monitoring velocity variations in the crust using earthquake doublets: An application to the Calaveras Fault, California, *J. Geophys. Res.*, *89*, 5719–5731, 1984.

Pujol, J., Comments of the joint determination of hypocenters and station corrections, *Bull. Seismol. Soc. Am.*, *78*, 1179–1189, 1988.

Pujol, J., Joint hypocentral location in media with lateral velocity variations and interpretation of the station corrections, *Phys. Earth Planet. Inter.*, *75*, 7–24, 1992.

Pujol, J., Application of the JHD technique to the Loma Prieta, California, mainshock-aftershock sequence and implications for earthquake location, *Bull. Seismol. Soc. Am.*, *85*, 129–150, 1995.

Pujol, J., An integrated 3D velocity inversion—Joint hypocentral determination relocation analysis of events in the Northridge area, *Bull. Seismol. Soc. Am.*, *86*, S138–S155, 1996.

Robertson, M.C., C.G. Sammis, M. Sahimi, and A.J. Martin, Fractal analysis of three-dimensional spatial distributions of earthquakes with a percolation interpretation, *J. Geophys. Res.*, *100*, 609–620, 1995.

Sambridge, M., and K. Gallagher, Earthquake hypocenter location using genetic algorithms, *Bull. Seismol. Soc. Am.*, *83*, 1467–1491, 1993.

Sambridge, M.S., and B.L.N. Kennett, A novel method of hypocentre location, *Geophys. J. R. Astron. Soc.*, *87*, 679–697, 1986.

Smith, E.G.C., An efficient algorithm for routine joint hypocentre determination, *Phys. Earth Planet. Inter.*, *30*, 135–144, 1982.

Spencer, C., and D. Gubbins, travel time inversion for simultaneous earthquake location and velocity structure determination in laterally varying media, *Geophys. J. R. Astron. Soc.*, *63*, 95–116, 1980.

Thurber, C.H., Earthquake locations and three-dimensional crustal structure in the Coyote Lake area, central California, *J. Geophys. Res.*, *88*, 8226–8236, 1983.

Thurber, C.H., Hypocenter-velocity structure coupling in local earthquake tomography, *Phys. Earth Planet. Inter.*, *75*, 55–62, 1992.

Viret, M., G.A. Bollinger, J.A. Snoke, and J.W. Dewey, Joint hypocenter relocation studies with sparse data sets–A case history: Virginia earthquakes, *Bull. Seismol. Soc. Am.*, *74*, 2297–2311, 1984.

Wald, L.A., L.K. Hutton, and D.D. Given, The Southern California Network Bulletin: 1990–1993 Summary, *Seismol. Res. Lett.*, *66*, 9–19, 1995.

Xie, J., Z. Liu, R.B. Herrmann, and E. Cranswick, Source processes of three aftershocks of the 1983 Goodnow, New York, earthquake: High resolution images of small symmetric ruptures, *Bull. Seismol. Soc. Am.*, *81*, 818–843, 1991.

Zeng, Y., K. Aki, and T.-L. Teng, Source inversion of the 1987 Whittier Narrows earthquake, California, using the isochron method, *Bull. Seismol. Soc. Am.*, *83*, 358–377, 1993.

P. M. Shearer, IGPP 0225, Scripps Institution of Oceanography, University of California, San Diego, La Jolla, CA, 92093-0225.

(Received March 21, 1996; revised September 19, 1996; accepted October 15, 1996.)